Scaling in film growth by pulsed laser deposition and modulated beam deposition

Sang Bub Lee
Department of Physics, Kyungpook National University, Daegu 702-701, Republic of Korea
(Received 2 April 2010; revised manuscript received 30 December 2010; published 13 April 2011)

The scalings in film growth by pulsed laser deposition (PLD) and modulated beam deposition (MBD) were investigated by Monte Carlo simulations. In PLD, an atomic pulse beam with a period t_0 were deposited instantaneously on a substrate, whereas in MBD, adatoms were deposited during a short time interval t_1 ($0 \leqslant t_1 \leqslant t_0$) within each period. If $t_1 = 0$, MBD will be identical to PLD and, if $t_1 = t_0$, MBD will become usual molecular beam epitaxy (MBE). Specifically, logarithmic scaling was investigated for the nucleation density reported for PLD, and the scaling of island density was studied regarding the growth for $0 < t_1 < t_0$ in MBD. It was found that the logarithmic scaling held for the nucleation density when growing islands were fractal-like but the quality of data collapsing became worse when islands were compact by adatom diffusion along the edges of islands. A crossover behavior from PLD growth to MBE growth was observed as t_1 increased. The phase diagram was also presented.

DOI: 10.1103/PhysRevE.83.041605 PACS number(s): 68.43.Jk, 68.55.A−, 05.45.Df

I. INTRODUCTION

Molecular beam epitaxy (MBE) is an important technique for fabricating nanostructures of high-purity crystals [1,2]. Many studies have been carried out on MBE, both theoretically, using mean-field-type rate equation analysis [3–5], scaling theories, and numerical simulations [6,7], and experimentally, using field ion microscopy [8], scanning electron microscopy [9], scanning tunneling microscopy [10–12], and reflection-high-energy-electron diffraction [10]. More recently, a pulsed laser deposition (PLD) was introduced and was increasingly used in the growth of multicomponent films and high-temperature superconducting films, as well as for the deposition of nanoparticles of various materials under a wide range of growth conditions [13–15]. The MBE and PLD techniques differ significantly from each other; in MBE, a steady-state flux F of adatoms is deposited on a flat substrate, whereas, in PLD, an atomic pulse beam of intensity I is deposited instantaneously. These two techniques possess their own characteristics and advantages; while MBE is the most popular and feasible technique of film growth, PLD yields, in many instances, a better layer-by-layer growth [16].

In this article, simulation results of the growth dynamics are presented for surfaces grown by a technique which is a combination of PLD and MBE, referred to as the modulated beam deposition (MBD). In MBD, IL^2 adatoms are deposited on a substrate of L^2 lattice sites during time t_1 within a period t_0, during which monomers deposited earlier simultaneously diffuse on a substrate. The film, then, undergoes relaxation for the rest of time in a given period before the next pulse is deposited. If $t_1 = t_0$, MBD is identical to MBE and, if $t_1 \to 0$, MBD becomes PLD. As t_1 increases from 0 to t_0, the scaling behavior of island density for MBD should cross over from the PLD behavior to the MBE behavior. One can, then, raise a question regarding which mechanism will dominate the growth for the cases of $0 < t_1 < t_0$.

The purpose of this article is twofold. First, the logarithmic scaling of the "nucleation density," discovered by Hinnemann, Hinrichsen, and Wolf [17], is investigated for the growth with $t_1 = 0$, i.e., for the PLD growth, particularly when growing islands are compact. It has been known that growing islands are compact when adatoms attached to island edges are activated to diffuse along the edges [18,19]. Similar logarithmic scaling was studied by Lam, Liu, and Woo [20]; however, unfortunately, these authors did not distinguish nucleation density from island density, and it was found that logarithmic scaling did not hold for the island density. The difference between the nucleation density and the island density will be described in Sec. II A. Second, in order to address the answer to the question raised in the preceding paragraph, the power-law behaviors of the saturated density of islands are investigated against the ratio of the diffusion-to-deposition rates and the normalized deposition time $\kappa = t_1/t_0$ for the growth by MBD, focusing on the case for $0 < t_1 < t_0$.

The MBD is similar to the deposition with a chopped flux proposed sometime ago [21], in which an incident flux F_i is chopped with a frequency f, so a steady-state flux is turned on during the time $0 < t < d/f$ and is off during the rest of time in a period. Although the turning-on-and-off procedure of the flux appears to be similar, this technique differs intrinsically from MBD. While the flux of an incident beam during the turning-on period is fixed in Ref. [21], the number of particles deposited within a period or, equivalently, the mean deposition flux is set to be constant in the present work. With these restrictions, the earlier model is better able to capture the essence of growth dynamics by chopped flux, whereas MBD is more suitable for the study of crossover behavior from PLD to MBE as the deposition time t_1 increases from 0 to t_0. It should be noted that, when $d/f \ll \tau_m$ (τ_m being the characteristic time), deposition with a chopped flux also reduces to PLD with the intensity $F_i(d/f)$, but d/f should not be too small and too large. (Note that if d/f is too small, i.e., if $d \to 0$, only a single atom will be deposited in each pulse and the growth will become similar to that of MBE [17].) On the other hand, MBD becomes precisely PLD when $t_1 \to 0$. The MBD technique also enables one to observe the scaling relations of island densities for various values of t_1 and the substrate temperature, as will be seen later.

Although the main interest of this work lies in the theoretical viewpoint, the MBD technique may also be applied experimentally in a way similar to that for the chopped flux by controlling the deposition flux in an appropriate way.

This article is organized as follows. In Sec. II, summary of the scaling theories and details of the Monte Carlo algorithm for MBD are presented. In Sec. III, results of the kinetic Monte Carlo simulations for the scaling of nucleation density in PLD and the scaling of island density in MBD are presented, together with relevant discussions. The summary and conclusions are given in Sec. IV.

II. THEORY AND METHODS

In this section, the key quantities and their scaling theories are summarized, and a simulation algorithm is presented.

A. Key quantities

For the purpose of the present work, it is necessary to calculate the nucleation density in PLD growth and the island density in MBD growth. It is assumed that clusters of size 2 or larger are immobile and form stable islands; thus, the critical island size is $i = 1$. (Note that the transient mobility of small clusters caused by impingement and energy transfer of incident particles which might be important in PLD for the case of supersaturated pulse has been ignored [22].) The nucleation density $n(\Theta)$ is the number of nucleation events per unit area in the first layer integrated over time up to the time at which coverage reaches Θ. The number of nucleation events is increased by 1 whenever a new island is nucleated either by deposition of an adatom on the nearest-neighbor site to a monomer or by encountering two monomers with each other by a surface diffusion and is never decreased even when two or more islands coalesce forming a larger island; therefore, it increases monotonically up to the coverage $\Theta = 1$ monolayer (ML) at which the first layer is completed. On the other hand, the island density ρ, i.e., the number of islands per lattice site, is increased by 1 whenever a new island is formed, is unchanged when monomers aggregate to existing islands, and is decreased when two or more islands coalesce. The island density, therefore, increases in the early-time region, reaches maximum in the steady-state region (often called aggregation region), and decreases in the coalescence region, when plotted against coverage. Although the nucleation density is not a familiar quantity in MBE like an island density, it is introduced in this work since the unusual logarithmic scaling was reported for it.

Both the nucleation density and the island density are sampled at the end of each pulse just before the new pulse is deposited. Thus, the minimal value of nucleation density, $n_{\min}$, is the one measured at the end of the first pulse and the maximal value, $n_{\max}$, is that calculated at $\Theta = 1$ ML.

B. Scaling theory

The fundamental quantities of primary interest in MBE are the monomer and island densities ρ_1 and ρ, which exhibit the power-law behaviors [5]:

$$\rho_1 \sim \Theta^{-\nu} R^{1-z}; \quad \rho \sim \Theta^{-\gamma} R^{-\chi}, \tag{1}$$

where R is the ratio of the monomer diffusion rate D and the adatom deposition rate F. In the steady-state region, in which adatoms aggregate to existing islands and island density remains in a steady state, the island density is a function of R alone. The power χ may be obtained from the rate equation analysis and is known to depend on the critical island size i, which is one less than the size of the smallest stable island, as $\chi = i/(i+2)$. For $i = 1$, it is more accurately known that $\chi = 2/(2 + d + d_f)$ [23], where d is the substrate dimension and d_f the fractal dimension of growing islands. Experimentally, the index χ is determined from the images obtained by various techniques mentioned earlier and, once χ is known, the free surface diffusion rate D_0 and the diffusion barrier E_0 are determined from the constant ρR^{χ} for various substrate temperatures. We will focus on how the index χ varies when the modulated deposition time t_1 varies within a period.

On the other hand, in PLD, the unusual scaling of the nucleation density was reported [17]. The nucleation density scaled by its maximum value, i.e., its value at the coverage $\Theta = 1$, $r = n(\Theta)/n(1)$, is known to yield the logarithmic scaling

$$\ln r = (\ln I) f(\ln \Theta / \ln I) \tag{2}$$

when growing islands are fractal. We will examine whether the same scaling relation holds for a particular case when growing islands are compact.

C. Simulation algorithm

Although the primary purpose of this work is to carry out kinetic simulations for PLD and MBD techniques, the simulation method for MBE is necessary for comparison purposes, prior to the other two.

In MBE, the dissociation barrier of adatoms from island edges is in general larger than the barriers of surface diffusion and edge diffusion. In metal-on-metal epitaxy such as Al/Al(111), Pt/Pt(100), and Fe/Cu(111), typical energy barrier is $E_{\rm dis} = 0.72$ eV, while surface diffusion and edge diffusion barriers are, respectively, $E_0 = 0.4$ eV and $E_e = 0.5$ eV [24–26]. Therefore, unless the substrate temperature is sufficiently high, the dissociation may be neglected and, thus, the present work is restricted to the irreversible growth. (For reversible growth with adatom detachment allowed, the scaling relation of island density is known to be significantly different from that for the irreversible growth; i.e., the exponent χ defined in Eq. (1) increases smoothly as the substrate temperature increases [27,28].) In all of the simulations in this work, the Schwoebel barriers are completely neglected, so the growth becomes layer by layer.

The atomic processes that should be considered in the irreversible growth are the deposition of FL^2 atoms per second, adatom diffusion on a substrate with a rate $N_0 D_0 e^{-E_0/k_B T}$, and edge diffusion with a rate $N_e D_0 e^{-E_e/k_B T}$, the prefactor $D_0 = 2k_B T/h$ being the frequency of atomic oscillation, N_0 and N_e being the numbers of monomers and edge-diffusion candidates, respectively, E_0 and E_e being the corresponding potential barriers, and T the substrate temperature. Adatoms attached to island edges with only one lateral bond are assumed to diffuse along island edges. In the experiments, atoms with two or more bonds may also diffuse but, since the potential barrier for such a diffusion is much higher than that of a one-bond diffusion, atoms with more than one lateral bond

are assumed to be stationary. The total rate is, thus, given as

$$N_{\rm tot} = FL^2 + N_0 D_0 e^{-E_0/k_BT} + N_e D_0 e^{-E_e/k_BT} = F[L^2 + R(N_0 + N_e r_e)] = F\mathcal{N}, \quad (3)$$

where the relations $\Delta E_e = E_e - E_0$, $r_e = e^{-\Delta E_e/k_BT}$, and $R = D/F$ ($D = D_0 e^{-E_0/k_BT}$) were used. Thus, the probabilities for deposition, diffusion, and edge diffusion are given, respectively, as

$$p_F = \frac{L^2}{\mathcal{N}}, \quad p_D = \frac{RN_0}{\mathcal{N}}, \quad \text{and } p_e = \frac{RN_e r_e}{\mathcal{N}}. \quad (4)$$

The evolution time should be accumulated by increasing $\Delta t = 1/N_{\rm tot}$ for each of the selected processes. In usual MBE growth, the coverage in ML unit is more frequently used for the evolution time. The time increment in an ML unit is $\Delta\tau = \Delta t/\Delta t_{\rm ML}$. Since FL^2 particles are deposited in a second, the time taken for deposition of an adatom is $\Delta t_{\rm atom} = 1/FL^2$ and, thus, the time taken for deposition of a monolayer is $\Delta t_{\rm ML} = \Delta t_{\rm atom} L^2 = 1/F$. Therefore, the time increment for each of the selected processes is in an ML unit $\Delta\tau = F/N_{\rm tot} = [L^2 + R(N_0 + N_e r_e)]^{-1}$. In the experiments, the coverage is measured for the evolution time; it is, therefore, sufficient to increase the evolution time by an amount of $\Delta\tau_{\rm atom} = 1/L^2$ whenever an adatom deposition is selected.

In PLD, since an atomic pulse beam is deposited with a period t_0 or, equivalently, with a frequency $1/t_0$, the mean deposition flux $F_{\rm av}$, defined by the flux when considering that IL^2 particles are deposited by a steady-state flux in a period, is given as $F_{\rm av} = I/t_0$. In an ML units, the period is given as

$$\tau_0 = t_0/\Delta t_{\rm ML} = I. \quad (5)$$

Therefore, a pulse of intensity I is deposited instantaneously and the film is subsequently left for relaxation during the time τ_0. Neglecting all hyperthermal nature of incident particles which may occur in PLD, the total rate of surface diffusion and edge diffusion is given as

$$N_{\rm tot} = N_0 D + N_e D r_e = F_{\rm av} R(N_0 + N_e r_e) = F_{\rm av} R\mathcal{N}_1, \quad (6)$$

where $R = D/F_{\rm av}$ in this case. Therefore, the probabilities for deposition and diffusion are given, respectively, as

$$p_D = \frac{N_0}{\mathcal{N}_1} \quad \text{and} \quad p_e = \frac{N_e r_e}{\mathcal{N}_1}. \quad (7)$$

During the relaxation time, the coverage does not increase; however, the mean elapsed time for each of the selected monomer diffusion and edge diffusion is $\Delta t = 1/(N_0 D + N_e D r_e)$. Therefore, the mean evolution time in ML unit is $\Delta t/\Delta t_{\rm ML} = [RN_0 + RN_e r_e]^{-1}$. However, the time increment between two consecutive hopping processes may not be constant and may vary stochastically and, therefore, it is increased by an amount

$$\Delta\tau = \frac{\ln(1/q)}{R(N_0 + N_e r_e)},$$

q being the random number between 0 and 1, for each hopping process. [Note that the mean of $\ln(1/q)$ is 1.]

In MBD, the situation is more complex than MBE or PLD growth. The mean deposition flux over the period is given by the similar way to PLD as $F_{\rm av} = I/t_0$ or, equivalently, $t_0 = I/F_{\rm av}$. Since $R = D/F_{\rm av} = Dt_0/I$, the surface diffusion rate can be written, in terms of R, as $D = RI/t_0$.

During the time interval $0 < t < t_1$, the total rate is

$$N_{\rm tot} = F_1 L^2 + D(N_0 + N_e r_e) = F_1 L^2 + (RI/t_0)(N_0 + N_e r_e), \quad (8)$$

where F_1 is the deposition flux during the time $0 < t < t_1$ and is related with the mean flux by $F_1 = F_{\rm av} t_0/t_1$. Since the pulse intensity can be written as $I = F_1 t_1$, Eq. (8) can be rewritten as

$$N_{\rm tot} = F_1[L^2 + \kappa R(N_0 + N_e r_e)] = F_1\mathcal{N}_2, \quad (9)$$

where $\kappa = t_1/t_0$ is the modulated deposition time scaled by a period. Therefore, the probabilities for deposition, surface diffusion, and edge diffusion are given, respectively, as

$$p_F = \frac{L^2}{\mathcal{N}_2}, \quad p_D = \frac{\kappa RN_0}{\mathcal{N}_2}, \quad \text{and} \quad p_e = \frac{\kappa RN_e r_e}{\mathcal{N}_2}. \quad (10)$$

During the time interval $t_1 < t < t_0$, since monomer diffusion and edge diffusion are activated, the total rate is the same as that given in Eq. (6) and the probabilities are precisely those given in Eq. (7).

The evolution time is updated by increasing by an amount

$$\Delta\tau = \frac{\kappa \ln(1/q)}{\xi L^2 + \kappa R(N_0 + N_e r_e)},$$

where $\xi = 1$ in an interval $0 < t < t_1$ and $\xi = 0$ in $t_1 < t < t_0$, for each selected process. The factor $\ln(1/q)$ is again to take into account the stochasticity of time increment between two consecutive processes.

III. RESULTS AND DISCUSSIONS

In all simulations, $F_{\rm av} = 0.1$ (atoms per site per second), $D_0 = 10^{13}$ (hops per atom per second) and $E_0 = 0.4$ eV were used. Typical morphologies obtained by MBD using $T = 400$ K and $I = 0.01$, at the coverage of $\Theta = 0.1$ ML, are compared in Fig. 1; the upper figures are for $E_e = \infty$, and the lower ones for $E_e = 0.5$ eV. [Note that $\kappa = 0$ and $\kappa = 1$ correspond to the PLD and MBE, respectively.]

A. Scaling of nucleation density for PLD

In order to examine whether logarithmic scaling holds for the nucleation density when an edge diffusion is activated in PLD, simulations were carried out on a square-lattice substrate of temperature $T = 440$ K, using $E_e = 0.5$ eV, $t_1 = 0$, and selected values of I, ranging $10^{-5} < I < 10^{-1}$. The selected size of the substrate was 1000×1000 but, when the finite-size effect is apparent, the same simulation was also carried out on a 2000×2000 lattice. For comparison, simulations were also carried out for $E_e = \infty$. When $E_e \to \infty$, edge diffusion is suppressed and islands formed are fractal which are similar in morphology to the diffusion-limited aggregations (DLAs); the growth is, therefore, referred to as the "fractal growth." In this particular case, the nucleation density is known to exhibit the unusual logarithmic scaling [17]. On the other hand, for a finite value of E_e, i.e., for $E_e = 0.5$ eV, the growing islands are compact and the growth is referred to as the "compact growth."

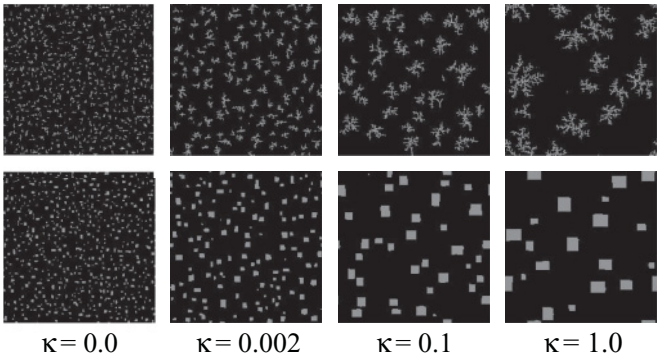

FIG. 1. Snap shot of the morphologies at the coverage of 0.1 ML, generated on a 200 × 200 square lattice by modulated beam deposition with $F_{\text{eff}} = 0.1$, $I = 0.01$, and $E_0 = 0.4$ eV, for selected values of the deposition time. The upper figures are for $E_e = \infty$, and the lower ones for $E_e = 0.5$ eV, both with the substrate temperature $T = 400$ K.

Diffusion of adatoms along island edges not only changes the morphology of growing islands from fractal-like to compact but it also yields islands of sizes 2 and 3 (dimers and trimers) to mobile by alternate hopping of adatoms along edges of the remaining atoms. Such small-cluster mobility is known to influence significantly the power-law behaviors of the densities of monomers and islands [28–30]. Therefore, in order to investigate the sole influence of the morphological changes of islands on the scaling of the nucleation density, it is necessary to suppress mobility of small islands. For this purpose, it is sufficient to inhibit edge diffusion of adatoms which are composed in dimers and trimers, because larger clusters quickly form stable, compact islands by edge diffusions. (Note that center of mass of compact tetramers and larger islands is immobile, even though adatoms on island edges diffuse along the edges.) It might also be interesting to compare both the results obtained with and without suppressing mobility to gain some insight into the influence of small-cluster mobility on the scaling of nucleation density in PLD and on the formation of islands in MBD. The nucleation density and island density are, thus, calculated with and without suppressing mobility of dimers and trimers.

It should be realized that there might be subtleties in defining "stable" islands when mobility of dimers and trimers are unsuppressed. The term island implies that clusters of adatoms are undissociable and immobile and, in this sense, dimers and trimers might not be considered islands for the case when mobility due to edge diffusion is unsuppressed. However, in the present work, since surface diffusion of dimers and trimers is neglected (i.e., diffusion barriers are considered to be infinite) and since mobility caused by edge diffusion of adatoms is in general much slower than that caused by surface diffusion, dimers and trimers are considered to be islands.

Plotted in Fig. 2 are $n_{\max}$ (upper set) and $n_{\min}$ (lower set) against I; it was determined that $n_{\max} = 0.340 I^{0.556}$ (circles) for the fractal growth and $n_{\max} = 0.334 I^{0.510}$ for the compact growth, both within the region $5 \times 10^{-5} \leqslant I \leqslant 5 \times 10^{-3}$, when mobility of dimers and trimers is suppressed (squares), and $n_{\max} = 0.189 I^{0.285}$ within the region of $2.5 \times 10^{-4} \leqslant I \leqslant 2.5 \times 10^{-2}$ when mobility is unsuppressed (triangles). Since

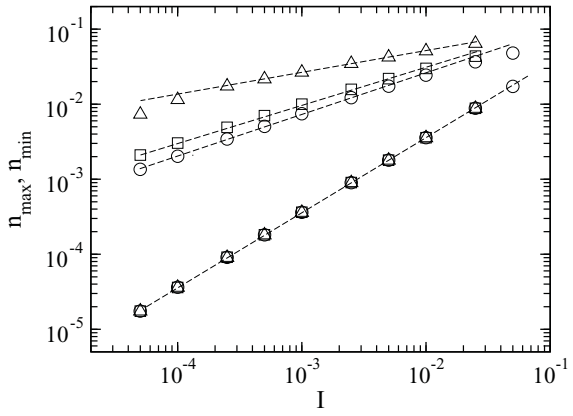

FIG. 2. The maximum and minimum values of nucleation density plotted against pulse intensity, generated using $F_{\text{eff}} = 0.1$, $E_0 = 0.4$ eV on a 1000 × 1000 substrate of temperature $T = 440$ K, in PLD. The circles are for the fractal growth, the squares for the compact growth using $E_e = 0.5$ eV with mobility of dimers and trimers suppressed, and the triangles for the compact growth with mobility unsuppressed. The upper sets are the maximum densities, and the lower sets overlapped one onto another are the minimum densities.

$n_{\min} \propto I$ for all cases, by plotting the nucleation density scaled by their maximum value, i.e., $r = n/n_{\max}$, against the coverage Θ on a double logarithmic scale, the right end point of each data set falls onto a single point, i.e., onto 1. Dividing the data by $\ln I$, the left end points also fall onto a single point; thus, both the right and left end points fall onto the same point. Such plots are shown in Fig. 3; the upper set of data are for the fractal growth, the lower set for the compact growth with mobility of dimers and trimers unsuppressed, and the middle set with the mobility suppressed. For the fractal growth, data for various pulse intensities fall on the same curve, indicating

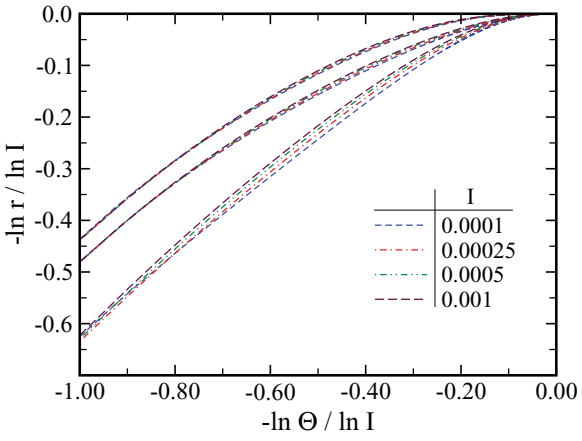

FIG. 3. (Color online) Plot of the logarithmically scaled nucleation density against the scaled coverage, for selected pulse intensities, generated using $F_{\text{av}} = 0.1$ and $E_0 = 0.4$ eV on a 1000 × 1000 square lattice of temperature $T = 440$ K, in PLD. The upper set is for the fractal growth and the remaining two sets for the compact growth with $E_e = 0.5$ eV, the middle one with edge diffusion of adatoms on dimers and trimers inhibited.

that logarithmic scale indeed holds for the nucleation density, as observed in Ref. [17].

For the compact growth with mobility of dimers and trimers suppressed, data approximately fall onto the same curve, though quality of collapse is not as good as for the fractal growth. Therefore, the morphology of islands does not appear to significantly influence the scaling of the nucleation density, unlike the earlier finding by Lam, Liu, and Woo [20]. It should be noted that they examined the scaling of island density, but the logarithmic scaling was reported for nucleation density [17]. On the other hand, when mobility of small islands is unsuppressed, data do not collapse. Since dimers and trimers move and aggregate to existing islands during the relaxation time $t_1 < t < t_0$, leaving large empty spaces on the substrate where nucleation may take place rather easily, mobility of small islands greatly enhances nucleation density, as was observed in Fig. 2. As pulse intensity increases, such enhancement becomes more significant and, accordingly, it appears to break the scaling.

In usual critical phenomena, it is known that logarithmic scaling is specific in the upper critical dimension. If the observed "unusual" scaling in two substrate dimensions is indeed logarithmic, the two-dimension will be a critical dimension and the scaling in one dimension might be of a power law or of a different type. In the earlier work in one dimension, it was found that similar logarithmic scaling was observed for both the island density (normalized by a different manner) and the nucleation density [31]. Based on the results, it was concluded that logarithmic data collapsing was accidental. Very recently, Barato, Hinrichsen, and Wolf carried out rate equation analysis on the nucleation density, and it was found that the scaling was not logarithmic in their analysis [32]. Therefore, although data appear to collapse in Fig. 3, such a scaling may be fortuitous. The same logarithmic scaling was also examined with the data for $\kappa = 10^{-4}$. Since this value of κ is sufficiently small so the growth for $10^{-4} \leqslant I \leqslant 10^{-3}$ is in the PLD regime, the logarithmic scaling should still hold if it is specific for the PLD growth. However, data did not fall on the same curve. This might be another indication that the logarithmic scaling observed for $\kappa = 0$ is not real in PLD growth.

B. Phase diagram

In order to observe how the growth dynamics varies as the pulse intensity and the modulated deposition time increases, the island density was calculated for selected values of I, ranging from 10^{-5} to 1, and κ from 0 (PLD) to 1 (MBE), all with $E_0 = 0.4$ eV and $E_e = \infty$.

Since the steady-state region becomes narrower as I increases, it was somewhat difficult to determine the steady-state region. Considering that island density, when plotted against the evolution time or coverage, increases in the early time, reaches maximum in the steady-state region and decreases sharply beyond it, the maximum value of ρ was assumed to be the steady-state density ρ_{ss}. Plotted in Fig. 4 are ρ_{ss}, obtained for a substrate temperature $T = 360$ K. For $\kappa = 0$, i.e., for pure PLD case, the island density increases with a power law $\rho_{ss} \sim I^{0.521}$ as shown with a thick dashed line. For $\kappa = 1$, since the probabilities in Eq. (10) are identical to those in Eq. (4) and do not depend on the pulse intensity, the island density remains the same as that for MBE, as presented by crosses in Fig. 4. For $\kappa > 0$, the island density for small I appears to follow the power-law behavior of pure PLD and then saturates as I further increases The steady-state values exhibit the power-law behavior $\rho_{ss} \sim \kappa^{-\alpha}$ with $\alpha \simeq 0.34$, which is close to the value of χ defined in Eq. (1). It should be noted that in the steady-state (aggregation) region the island density scales as $\rho_{ss} \propto R^{-\chi}$, with $\chi = 2/(2 + d + d_f)$, which is $\chi \simeq 0.35$ for the fractal islands of the fractal dimension similar to that of DLA, $d_f \simeq 1.7$ [33,34], and $\chi = \frac{1}{3}$ for the compact islands [35]. Since $\alpha = \chi$, one can write

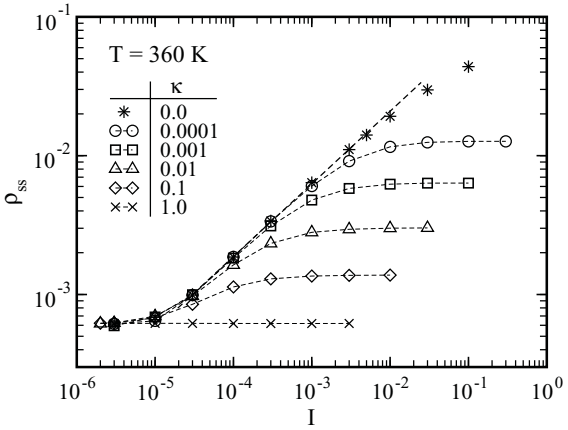

FIG. 4. The steady-state (maximum) values of island density, obtained from MBD growth with $F_{av} = 0.1$, $E_0 = 0.4$ eV, and $E_e = \infty$, plotted against the intensity of incoming flux for selected values of the modulated deposition time.

$$\rho_{ss} \propto (\kappa R)^{-\alpha}, \tag{11}$$

implying that, for a finite and not too small I, the growth dynamics is similar to that of MBE but with the reduced ratio of the diffusion-to-deposition rates κR (we refer to this as "extended MBE (EMBE) growth"). This observation is precisely what one can expect by comparing the probability distributions in Eq. (10) with the MBE probabilities in Eq. (4). Intuitively, increasing κ reduces the effective deposition flux and, accordingly, enhances R within the region $0 < t < t_1$. However, this argument is valid only when monomers disappear instantaneously as soon as they arrive on the substrate and nothing happens during the relaxation time $t_1 < t < t_0$. As an example, for sufficiently small κ, the effective deposition flux is very large when flux is on, and the monomer density increases rapidly. When flux is off and the substrate is under relaxation, monomers nucleate and island density increases during the relaxation. This situation is similar to that for the PLD growth and the scaling relation in Eq. (11) is no longer valid.

From Fig. 4, it is clear that, for small values of κ, data exhibit three different phases; (i) the MBE phase for $I \leqslant 10^{-5}$, (ii) the PLD phase in which data follows the PLD power-law behavior, and (iii) the EMBE phase. Although the boundary between the PLD and EMBE phases are unclear and determination of it from the data may be subjective, the phase diagram of the MBD growth can be drawn as in Fig. 5. For different substrate

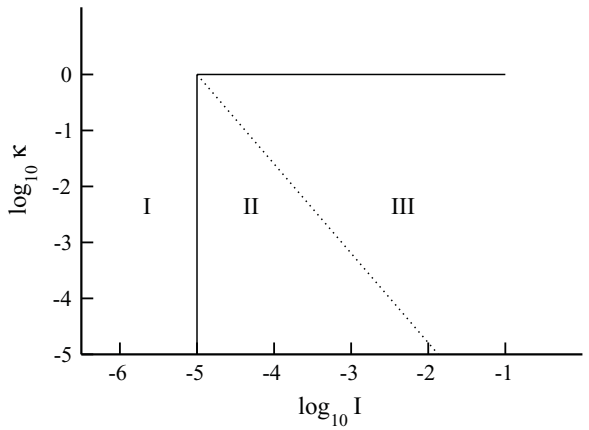

FIG. 5. Phase diagram of the MBD growth for the substrate temperature $T = 360$ K. The regions specified by I, II, and III correspond, respectively, to MBE, PLD, and EMBE. The boundary line between PLD and EMBE (dotted line) was drawn from Fig. 4 by connecting the points for various values of κ at which data begin to deviate from the PLD power-law behavior.

temperatures, the boundaries of different phases may be shifted but the diagram is qualitatively similar.

C. Scaling of island density for MBD

In Sec. III B, it was found that the steady-state island density depended on κ and R via the relation $\rho_{ss} \propto \kappa^{-\alpha} R^{-\chi}$, with $\alpha = \chi$. According to the phase diagram in Fig. 5, the same relation should hold for any finite value of I within a certain range of κ. Then, the data of scaled island density $\rho(\kappa R)^{\chi}$ for various values of κ and R would fall on the single curve in the aggregation region when plotted against the coverage. The value of R is given as $R = D/F_{\text{eff}} = 10^{14} e^{-E_e/k_B T}$ for the values of D_0 and F_{av} selected in this study and, thus, varies by varying the substrate temperature.

Plotted in Fig. 6 are the steady-state island densities with respect to the fractal growth ($E_e = \infty$) for $T = 400$ K (squares) and $T = 440$ K (circles) and $I = 0.0005$, for selected

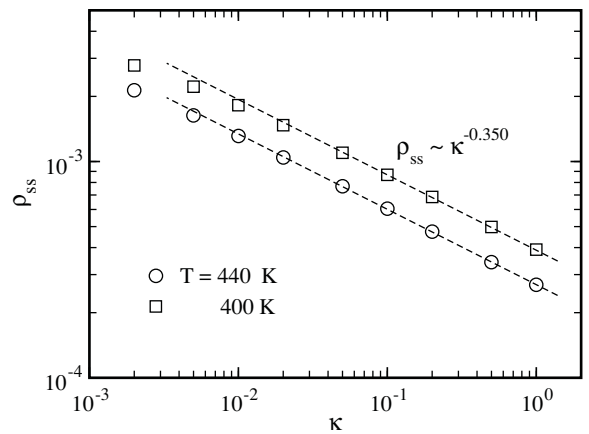

FIG. 6. Plot of the density of islands in the aggregation region against the modulated deposition time, generated using $F_{\text{eff}} = 0.1$, $I = 0.0005$, $E_0 = 0.4$ eV, and $E_e = \infty$, for two selected values of the substrate temperature in MBD.

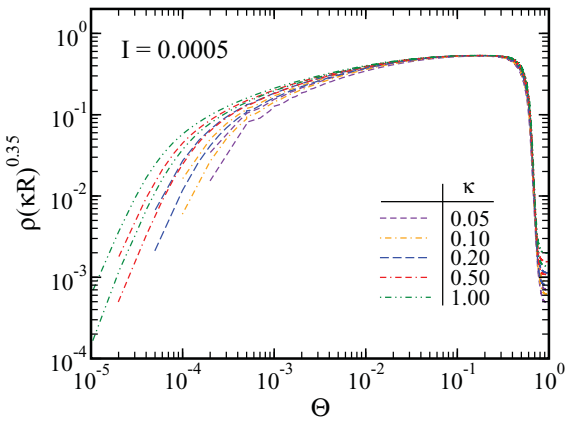

FIG. 7. (Color online) Plot of the scaled densities of islands, $\rho(\kappa R)^{\chi}$, against the coverage, generated using $E_{\text{eff}} = 0.1$, $I = 0.0005$, $E_0 = 0.4$ eV, and $E_e = \infty$, for two different values of the substrate temperature. The upper data for the same type lines are for $T = 440$ K and the lower ones for $T = 400$ K.

values of κ. (Note that, in this case, the period of deposition is $t_0 = I/F_{\text{av}} = 5 \times 10^{-3}$ sec or, equivalently, the frequency is 200 Hz.) Both data sets appear to exhibit power-law behaviors with the same power of $\alpha \simeq 0.350$ within the region $\kappa \geqslant 0.03$ which is indeed close to the value $\chi \simeq 0.35$. Figure 7 shows the simulation data for $\rho(\kappa R)^{\chi}$, with $\chi = 0.35$, plotted against the coverage; data in the aggregation region ($0.05 \leqslant \Theta \leqslant 1.0$) fall onto the same curve.

For the compact growth using $E_e = 0.5$ eV, with mobility of dimers and trimers suppressed, similar power-law dependance of ρ_{ss} on κ is observed in the aggregation region but with the power $\alpha \simeq 0.33$, which is again close to the known value of $\chi = \frac{1}{3}$ for the compact growth. The scaling plot is displayed in Fig. 8; the inset is the steady-state densities of islands

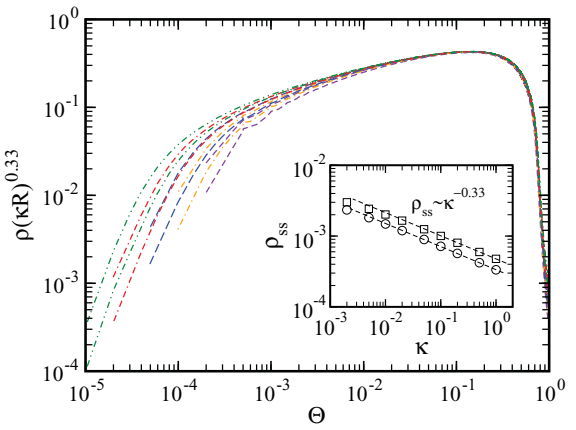

FIG. 8. (Color online) Plot of the scaled densities of islands, $\rho(\kappa R)^{\chi}$, against the coverage, generated using $E_{\text{eff}} = 0.1$, $I = 0.0005$, $E_0 = 0.4$ eV, and $E_e = 0.5$ eV, with mobility of dimers and trimers suppressed, for two different values of the substrate temperature. The types of lines are for the same deposition times as those in Fig. 7. The inset shows the steady-state densities of islands for $T = 440$ K (circles) and $T = 400$ K (squares), with the dashed lines the regression fits.

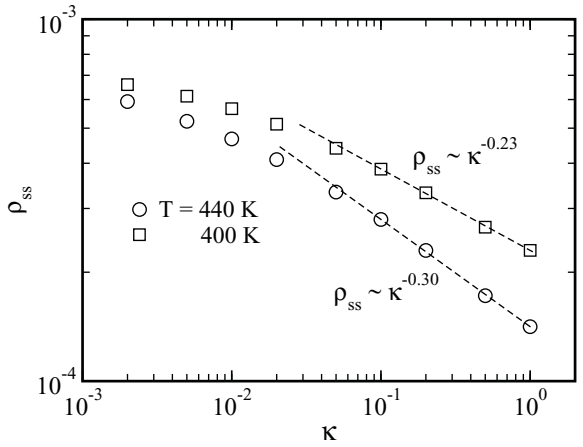

FIG. 9. Plot of the density of islands in the aggregation region against the modulated deposition time, generated using $F_{\text{eff}} = 0.1$, $I = 0.0005$, $E_0 = 0.4$ eV, and $E_e = 0.5$ eV, without suppressing the mobility of dimers and trimers, for two selected values of the substrate temperature in MBD.

plotted against the scaled deposition time, for two substrate temperatures, $T = 440$ K (circles) and $T = 400$ K (squares). Again, the data for various values of κ and for different temperature values fall onto the same curve. The scaling plots for both fractal growth and compact growth indicate that the power-law behavior of the steady-state densities of islands with respect to the MBD growth is identical to that of MBE but with a reduced deposition flux.

For the compact growth, without suppressing the mobility of dimers and trimers, it was found that, in the region of $0.1 \leqslant \kappa \leqslant 1$, $\rho \propto \kappa^{-0.30}$ for $T = 440$ K and $\rho \propto \kappa^{-0.23}$ for $T = 400$ K, as shown in Fig. 9; thus, the scaling relation becomes $\rho_{ss} \propto \kappa^{-\alpha} R^{-\chi}$, with $\chi \simeq \frac{2}{5}$ [28] and α being dependent on the substrate temperature. Therefore, a universal scaling law does not exist for various substrate temperatures, when dimers and trimers are mobile. Failure of the universal scaling law is attributed to the fact that small clusters diffuse during the relaxation time $t_1 < t < 1$ in each period and, therefore, island density significantly decreases. As the substrate temperature increases, the mobility increases and, accordingly, island density decreases more rapidly as κ increases. This results in the power α being dependent on the substrate temperature or, equivalently, on the ratio of the diffusion-to-deposition rates, yielding a failure of the universal scaling over the substrate temperature. Indeed, data of the island density within the power-law region of κ collapsed onto the same value in the aggregation region for each substrate temperature, but those for different temperatures did not fall on the same curve. The scaling region became much narrower, compared with the other two cases discussed earlier (not shown).

The results in this work may be compared with those of the earlier work by Jensen and Niemeyer [21]. While in the earlier work the deposition of a constant flux F_i is turned on during $0 < t < d/f$ in each period of frequency f, in this work it is turned on during $0 < t < t_1$ in each period; therefore, $1/f$ and d correspond, respectively, to t_0 and κ. When plotting the island density against f/d, three distinct regions were observed: (i) $\tau_m \ll d/f$, (ii) $\tau_m \gg d/f$, and (iii) $\tau_m \gg 1/f$, τ_m being the time after which the monomer density attains its steady-state value after each deposition process in each period. In region (i), the steady-state island density grows as $\rho_{ss} \sim R^{-\chi}$, which is precisely the island density of MBE growth. On the other hand, in (iii), i.e., in the high-frequency region, it was given as $\rho_{ss} \sim R^{-\chi} d^{\chi}$; i.e., island density increased as d increased. It is obvious that ρ_{ss} increases as d increases because more particles are deposited in a period. However, in the present work, the island density decreased as κ increased, as was seen in Fig. 6, because the effective flux F_1 decreased as κ increased. The difference is clearly attributed to the difference of the two growth models. Moreover, it was not clear from the earlier results that the island density was similar to that of PLD in the $d \to 0$ limit. The present data, however, exhibited precisely those of PLD in the $\kappa \to 0$ limit and those of MBE in the $\kappa \to 1$ limit. Therefore, MBD better presents the crossover behavior from PLD to MBE as κ increases.

IV. SUMMARY AND CONCLUSIONS

In summary, the unusual logarithmic scaling of nucleation density was found to hold for both the fractal growth and the compact growth with mobility of dimers and trimers suppressed, but the quality of data collapsing for the latter case is not as good as for the former case, unlike the results for island density by Lam, Liu, and Woo. On the other hand, when dimers and trimers are mobile by consecutive edge diffusions of adatoms, such a scaling did not hold. The logarithmic scaling was also investigated for $\kappa \ll 1$, for which the growth dynamics is expected to be similar to that of PLD within the region of small values of I, but data did not scale. Based on these observations and the earlier results, it is concluded that the logarithmic scaling observed in PLD is not real but appears to be accidental.

For MBD growth, the steady-state density of islands exhibited the power-law behavior $\rho_{ss} \sim \kappa^{-\alpha} R^{-\chi}$, with $\alpha = \chi$ when mobility of dimers and trimers is suppressed. The scaling plot exhibited excellent data collapsing in the steady-state region, for both the fractal growth and the compact growth. From the results, it is concluded that the growth mechanism of MBD is similar to that of the usual MBE but with different deposition rates, as long as the modulated deposition time is not too small. (If it is too small, then the growth appears to be similar to the PLD growth.) We have presented the results for the two substrate temperatures. The substrate temperature is associated with the monomer hopping rate via $D = D_0 e^{-E_0/k_B T} \simeq 9.12 \times 10^7$ [hops per second per atom] for $E_0 = 0.4$ eV and $T = 400$ K; therefore, $R \approx 10^9$, which is the value certainly accessible by experiments. With this value, monomers disappear instantaneously as soon as they arrive on the substrate and nothing happens during the relaxation time. If R is not large enough, e.g., if $R \sim 10^6$ or smaller, the scaling relation in Eq. (11) will no longer be valid. It might be interesting to observe whether such scaling regions exist for much smaller substrate temperatures, and such a problem is left for future study.

On the other hand, when small clusters are mobile, the power-law region of the saturated density of islands becomes

narrower and the universal power-law behavior for various substrate temperatures was not observed, implying that mobility of small clusters significantly influences the power-law behaviors for both the PLD and MBD growth.

ACKNOWLEDGMENTS

This work was supported in part by the Korea Science and Engineering Foundation Grant (Grant No. 2008-0058988). The author is grateful for the support.

[1] J. W. Matthews, *Epitaxial Growth* (Academic, New York, 1975).
[2] A. Pimpinelli and J. Villain, *Physics of Crystal Growth* (Cambridge University Press, Cambridge, UK, 1998).
[3] M. von Smoluchowski, Z. Phys. Chem. **17**, 557 (1916).
[4] M. C. Bartelt and J. W. Evans, Phys. Rev. B **46**, 12675 (1992).
[5] J. G. Amar, F. Family, and P.-M. Lam, Phys. Rev. B **50**, 8781 (1994).
[6] F. Family and P. Meakin, Phys. Rev. Lett. **61**, 428 (1988).
[7] J. G. Amar and F. Family, Phys. Rev. Lett. **74**, 2066 (1995).
[8] S. C. Wang and G. Ehrlich, Surf. Sci. **239**, 301 (1990).
[9] K.-S. Hwang, Y.-S. Jeon, B.-A. Kang, K. Nishio, T. Tsuchiya, J.-H. An, and B.-H. Kim, J. Korean Phys. Soc. **46**, 521 (2005).
[10] J. A. Stroscio, D. T. Pierce, and R. A. Dragoset, Phys. Rev. Lett. **70**, 3615 (1993).
[11] J.-S. Ha, K.-H. Park, Y.-J. Ko, and K.-W. Park, J. Korean Phys. Soc. **39**, 436 (2001).
[12] V. Cherepanov, S. Filimonov, J. Myslivecek, and B. Voigtländer, Phys. Rev. B **70**, 085401 (2004).
[13] D. H. Lowndes, D. B. Geohegan, A. A. Puretzky, D. Norton, and D. G. Rouleau, Science **273**, 898 (1996).
[14] D. B. Chrisey and G. K. Hubler, *Pulsed Laser Deposition of Thin Films* (Wiley, New York, 1994).
[15] W. Marine, L. Patrone, B. Luk'yanchuk, and M. Sentis, Appl. Surf. Sci. **154-155**, 345 (2000).
[16] J. Shen, Z. Gai, and J. Kirschner, Surf. Sci. Rep. **52**, 163 (2004).
[17] B. Hinnemann, H. Hinrichsen, and D. E. Wolf, Phys. Rev. Lett. **87**, 135701 (2001); Phys. Rev. E **67**, 011602 (2003).
[18] G. S. Bales and D. C. Chrzan, Phys. Rev. B **50**, 6057 (1994).
[19] F. Family and J. G. Amar, Mater. Sci. Eng. B **30**, 140 (1995).
[20] P.-M. Lam, S. J. Liu, and C. H. Woo, Phys. Rev. B **66**, 045408 (2002).
[21] P. Jensen and B. Niemeyer, Surf. Sci. **384**, L823 (1997); N. Combe and P. Jensen, Phys. Rev. B **57**, 15553 (1998).
[22] E. Vasco, New J. Phys. **8**, 253 (2006).
[23] M. Schroeder and D. E. Wolf, Phys. Rev. Lett. **74**, 2062 (1995).
[24] P. J. Feibelman, Phys. Rev. Lett. **58**, 2766 (1987).
[25] S. Liu, Z. Zhang, J. K. Norskov, and H. Metiu, Surf. Sci. **321**, 161 (1994).
[26] T. J. Raeker and A. E. DePristo, Surf. Sci. **317**, 283 (1994).
[27] C. Ratsch, A. Zangwill, P. Šmilauer, and D. D. Vvedensky, Phys. Rev. Lett. **72**, 3194 (1994).
[28] S. B. Lee and B. C. Gupta, Phys. Rev. B **62**, 7545 (2000).
[29] S. Liu, L. Bönig, and H. Metiu, Phys. Rev. B **52**, 2907 (1995).
[30] M. C. Bartelt, S. Gunther, E. Kopatzki, R. J. Behm, and J. W. Evans, Phys. Rev. B **53**, 4099 (1996).
[31] S. B. Lee, Phys. Rev. E **67**, 012601 (2003).
[32] A. C. Barato, H. Hinrichsen, and D. E. Wolf, Phys. Rev. E **77**, 041607 (2008).
[33] L.-H. Tang, J. Phys. I **3**, 935 (1993).
[34] S. B. Lee, J. Korean Phys. Soc. **47**, 577 (2005).
[35] S. B. Lee, Phys. Rev. B **73**, 035437 (2006).